ORIGINAL ARTICLE

C-phycoerythrin production from *Anabaena* sp. BTA 903: Optimization, production kinetics, thermodynamic, and stability analysis

Pinku Chandra Nath[1] · Tarun Kanti Bandyopadhyay[2] · Nibedita Mahata[3] · Onkar Nath Tiwari[4] · Md. Nazneen Bobby[5] · Mikkili Indira[5] · Biswanath Bhunia[1]

Abstract

The cyanobacterium BTA 903 isolated from Manipur state of India was identified as *Anabaena* sp. after phylogenetic analysis. BTA 903 contained ash (5.84% w/w), carbohydrate (42.36% w/w), protein (33.46% w/w), lipid (16.46% w/w), and moisture (1.88% w/w), respectively. BTA 903 required 0.3 M glycine and 5 mM sodium glutamate as supplements in BG 11 media in order to achieve the highest amount of cell growth along with C-phycoerythrin (PE) production. The light intensity of 6 k Lux, along with a photoperiod of 14:10 (L:D) was revealed to be optimal for increased productivity. The yields of C-phycoerythrin, C-phycocyanin, allophycocyanin, chlorophyll-a, and ammonia excretion after 30 days of incubation of *Anabaena* sp. were 49.96, 27.53, and 30.39, 6.9, and 31.2 mg per gram of biomass, respectively. The biomass productivity of *Anabaena* sp. BTA 903 was found to be 39 mgL^{-1} day^{-1} after 30 days of incubation. PE from *Anabaena* sp. was extracted using 0.05 M phosphate buffer (pH-7). The deactivation process of PE was investigated using a first-order kinetic model. The rate constant (k_d) was found to be in the range of 0–0.01 h^{-1} when the deactivation study was carried out at pH 7 and temperatures ranging from 10 to 30 °C. The highest level of PE deactivation was found at 80 °C and pH 12 due to a higher k_d value (0.671 h^{-1}). At pH 7, the highest Gibb's free energy for PE was found to be 103.70–115.69 kJ/mol. PE's pH and thermal tolerances suggested that it could be used for industrial applications.

Keywords *Anabaena* sp. · C-phycoerythrin · Rate constant · Production kinetics · Stability analysis

1 Introduction

Cyanobacteria produce a variety of biologically active compounds in the industry due to their inherent ability to synthesize a wide range of chemically distinct biochemical compounds. It is evident that natural reddish colourants have a growing market in the beverage manufacturing industry. Because these colourants are extremely rare in nature, manufacturers rely on synthetic colourants. Therefore, the food industry is looking for natural reddish colourants that can be

✉ Onkar Nath Tiwari
  ontiwari1968@gmail.com

✉ Biswanath Bhunia
  bbhunia@gmail.com

  Pinku Chandra Nath
  nathpinku005@gmail.com

  Tarun Kanti Bandyopadhyay
  tarunkantibanerjee0@gmail.com

  Nibedita Mahata
  nibedita.mahata@bt.nitdgp.ac.in

  Md. Nazneen Bobby
  slh41025@gmail.com

  Mikkili Indira
  indiramikkili@gmail.com

[1] Department of Bio Engineering, National Institute of Technology, Agartala-799046, India

[2] Department of Chemical Engineering, National Institute of Technology, Agartala-799046, India

[3] Department of Biotechnology, National Institute of Technology Durgapur, Durgapur-713209, India

[4] Centre for Conservation and Utilisation of Blue Green Algae, Division of Microbiology, ICAR-Indian Agricultural Research Institute (ICAR-IARI), New Delhi-110012, India

[5] Department of Biotechnology, Vignan's Foundation for Science Technology and Research, Guntur -522213, Andhra Pradesh, India

stable for a more extended period in a robust condition. Protein is the second most abundant nutrient in most cyanobacteria. PE is a naturally occurring reddish colourant, one of the light-harvesting proteins available in cyanobacteria [1]. A variety of factors, including nutritional limitation, photoperiods, and light intensity, are required for cyanobacterial growth and PE production [2]. Furthermore, the majority of pigments are produced in proportion to the amount of biomass produced. As a result, biomass production must be optimized in order to boost PE productivity. Furthermore, while large-scale PE production was carried out in the industry, it was found that kinetic studies of PE production are critical for reactor design [3, 4].

The homogenization and freezing–thawing methods are extensively used to extract PE from algal biomass. Although these methods produce significantly more PE, the active form of PE was lost due to harsh techniques. Extraction and purification of PE have been critical tasks due to their thermolability [5]. Aqueous two-phase systems were used as an alternative method to separate thermolabile biomolecules because they provide an aqueous environment and mild operating conditions. Hence the molecule's native conformation will be preserved during separation. Temperature-dependent two-phase aqueous micellar systems have recently drawn interest in the separation of thermolabile biomolecules due to their biocompatibility and low cost. The proper temperature manipulation resulted in the formation of two phases of this system. When the temperature rises above the cloud point, two distinct macroscopic phases emerge. This system can be further manipulated by adding salts, cosurfactants, or ionic liquids [6]. Deep eutectic solvents are another approach that is task specific. They are also more effective, simple to synthesize, and biodegradable. Furthermore, while the extraction is being performed, this system maintains the buffer condition for the active bioproducts. The reaction of an organic acid with quaternary ammonium salts or sugar molecules yields protic deep eutectic solvents. Their acidic nature, combined with the ability to form aqueous two phases, makes them a better approach for disruptive purification medium for PE [5]. The purification of PE was carried out using ammonium sulfate precipitation followed by various chromatography methods [7].

Since radical scavenging, anti-inflammatory, and hepatoprotective properties are three important health-promoting characteristics found in PE, its use in the food and pharmaceutical industries is increasing [8, 9]. The vivid bright colour of PE is one of the reasons for its increased demand as an additive in the food industry. The primary disadvantage of PE has been observed to be its instability over a wide pH range and at higher temperatures. Several physicals (temperature and pH) and chemical parameters have been found to influence PE stability [10]. To be used effectively in a variety of industries, PE must be stable at high temperatures and over a wide pH range [11]. As a result, new sources of PE must be sought in order to achieve significantly improved stability when used in a wide pH range and at high temperatures [12]. PE's stability is calculated by measuring the amount of colour that remains after being exposed to various environmental conditions [13]. PE stability analysis is critical for biotechnological applications because it provides a complete physical understanding of its three-dimensional structure [14]. According to our current knowledge, only a limited research work has been reported on the deactivation study of PE. The majority of studies have focused on the biochemical characteristics of PE; however, there has been little research done on its thermodynamic behaviour under various environmental conditions. As the thermodynamic behaviour of PE has the potential to affect stability, the investigation of deactivation studies of PE has been highlighted in this manuscript.

In the present study, various process factors were optimized in order to achieve a higher PE yield from BTA-903. To identify the BTA 903, microscopic and molecular characterization were performed. Biochemical characterization of BTA 903 was performed in order to understand the types of bioproducts that could be produced from it. Furthermore, the batch kinetic investigation of PE production was investigated in order to ascertain various kinetic parameters required for reactor design. Furthermore, the stability analysis of PE was performed better to understand the effects of pH and temperature on it.

2 Material and methods

2.1 Isolation of BTA-903

The cyanobacterium employed in this investigation was isolated from semisolid samples obtained from rice fields in Manipur, India. The spatula was used to collect the samples, which were then stored in plastic bottles. While the collected sample was diluted with distilled water, the ratio of 1:2 w/v was maintained. While sampling was taking place, a global positioning system device helped to pinpoint the exact position of the sample collecting location. BTA 903 was chosen from among other strains for this study due to its high PE synthesis yield when grown in BG 11 liquid media. The pure strain was produced in BG 11 solid media using the striking method. The aforementioned pure strain was registered to IBSD-Imphal, a National Algae Repository financed by DBT, Government of India, with accession id of BTA-903. The maintenance of cyanobacterium BTA 903 was carried out on BG-11 medium [15]. BTA 903 was subcultured every one-week interval in BG 11 liquid media in order to achieve a healthy cyanobacterium strain.

2.2 Morphological and molecular characterization of BTA 903

The BTA 903 was identified through molecular characterization and morphology. The BTA 903's morphology was investigated using a trinocular Nikon Eclipse 80i

research microscope with 63X objectives. 16S rRNA technique was used for molecular characterization [16]. The gene bank available at the NCBI site was used to understand the level of similarity of the gene sequence of 16S rDNA present in BTA 903 using a nucleotide BLAST search [17]. The BTA 903 was identified by comparing its 16 s rDNA sequence to those of other cyanobacterium in the database. MEGA 7.0 software was used to construct a maximum likelihood phylogenetic tree and determine evolutionary distance bootstrap values using the Jukes-Cantor model of neighbour-joining [18].

2.3 Cultivation of BTA 903

The preparation of seed culture of BTA 903 was carried out in a 500-ml Erlenmeyer flask where 100 ml BG 11 media was taken. The inoculation of a single loop of pure BTA 903 cultures, which was previously grown, was taken in BG 11 liquid media having pH of pH-6.8, and incubation was carried out at 28 °C for 7 days. The intensity of light and a day/night ratio were maintained 4 k Lux and 12:12, respectively. After a 24-h interval, the media was manually agitated to ensure uniform mixing of the media components. After seed culture preparation, 5% fresh seed culture was inoculated into 100 ml of BG 11 media in a 500-ml Erlenmeyer flask. The culture was grown for thirty days in the same conditions described in seed culture preparation. The samples were taken every 2 days and analysed to determine the biomass and PE production level using the previously described protocol [19].

2.3.1 Determination of optimum level of glycine, sodium glutamate, light intensity, and photoperiod on biomass and PE production

Two media components, glycine and sodium glutamate, and two process parameters, light intensity and photoperiod, were optimized to better understand their effects on cyanobacterial growth and productivity of PE. Here, the level of glycine was optimized first, followed by sodium glutamate, light intensity, and photoperiod. The level of biomass and PE production was assessed using previously described protocol [19]. Glycine was added to the BG liquid medium at various concentrations ranging from 0.1 M to 0.4 M, and sodium glutamate was added at levels ranging from 2.5 M to 10 M to determine the optimum level of them on PE growth and productivity. To better understand the role of light intensity and photoperiod on PE growth and productivity, light intensity was varied from 4 k Lux to 8 k Lux, and photoperiod was adjusted to 16:8 (light/dark), 14:10 (light/dark), 12:12 (light/dark), and 8:16 (light/dark). The higher amount of biomass and PE were the factors taken to determine the optimum level of all

parameters. When cultures were grown for thirty days in the same conditions described in seed culture preparation, biomass and PE production in BG liquid media without any nutrients were presumed as controls. Every experiment was done in triplicate.

2.4 Determination of PE

After 30 days of incubation, the cells were separated by centrifugation at 6500 g for 10 min at 4 °C. The harvested cells were homogenised using REMI Lab Homogeniser RQ-127A/D with 5 ml of phosphate buffer (0.05 M) having pH-7 was taken. To remove cell debris, the homogenised cells were centrifuged at 6500 g for 10 min at 4 °C, and the supernatant was used to determine the PE content [20]. All experiments were performed in triplicate.

2.4.1 Growth and PE production kinetics

Initially, 100 ml of sterilized BG liquid media was prepared in a 500-ml Erlenmeyer flask, and 5% of freshly prepared seed culture of BTA 903 was added. The incubation was carried out at 28 °C for 30 days. The optimal levels of glycine and sodium glutamate were also added to BG 11 liquid media, and the light intensity and photoperiod obtained in previous experiments were kept. The withdrawal of samples was carried out at two-day intervals and the analysis of biomass and PE production was performed. Equation (1) was used to calculate the specific growth rate ($\mu_{BTA\,903}$) of BTA 903 [21], where, $X_{BTA\,903}$ is biomass concentration (gL^{-1}), and $\mu_{BAT\,903}$ is the specific growth rate of BTA 903 (1/h).

$$\mu_{BTA903} = \frac{1}{X_{BTA903}} \frac{dX_{BTA903}}{dt} \qquad (1)$$

In the batch study, the kinetic nature of PE production was represented by the Leudeking-Piret (LP) model [22]. The specific production rate (ν_{PE}) of PE was calculated using Eq. (2). It is evident from Leudeking-Piret model that the specific PE production rate (ν_{PE}) depends on the specific growth rate ($\mu_{BAT\,903}$) of BTA 903 (Eq. 3)

$$\nu_{PE} = \left(1/X_{BTA903}\right)\left(\frac{dPE}{dt}\right) \qquad (2)$$

$$\nu_{PE} = a\mu_{BTA903} + \beta \qquad (3)$$

where α and β represent the growth-associated constant and the non-growth-associated constant, respectively. The specific production rate (ν_{PE}) of PE and specific growth rate ($\mu_{BAT\,903}$) of BTA 903 were calculated in each time interval.

2.5 Analysis of cellular components, PBPs, chlorophyll-a, ammonia excretion of BTA 903

The proportion quantity of lyophilized BTA 903 cell was measured to determine the major cellular components. The amount of ash, moisture, carbohydrate, protein, and lipid content present in BTA 903 were measured. Lyophilized cells were heated in a furnace at 550 °C to determine ash content, and the weight difference before as well as after heating was measured. To determine the quantity of moisture, the sample was heated at 105 °C for one day in the dry oven. The weight difference between before and after heating was calculated [23]. Total protein content was determined using the Lowry method, with bovine serum albumin (BSA) serving as a standard [24]. To estimate total carbohydrate content, Anthrone method was used with glucose serving as a standard [25]. To estimate lipid content, gas chromatography was used [26]. The samples' phycobiliprotein, chlorophyll-a and ammonia excretion content was determined using a previously described protocol [9, 19]. All experiments were conducted in triplicate.

2.6 Thermodynamics and stability of PE

The thermal and pH stability of PE was investigated at various temperatures and pH combinations for 1 h. The pH range was maintained from 2 to 12 using Britton-Robinson buffer

to achieve a stable pH range. Thermal deactivation of PE was investigated at each pH with temperatures ranging from 10 to 80 °C. After a 15-min interval, the remaining PE content in the withdrawn sample was determined [9, 19]. The PE incubated at 4 °C and pH 7 in Britton-Robinson buffer was used as a control.

3 Results and discussion

3.1 Morphological, and molecular characterization of BTA 903

BTA 903 was isolated from semisolid samples obtained from rice fields in Manipur, India (Altitude: 782 m,N 24°52´09.0´´E094°1´12.9´). BTA 903 was identified using morphological analysis and molecular characterization. The discrete biological aspect of individual strain and model arrangements that take into account identification methods in biology were employed. Figure 1A shows optical microscopic images of isolated BTA 903 at 63X magnification. The figure depicts cyanobacterium with various differentiations within the framework, displaying physiological and structural complexity. BTA 903 has straight filaments or coiling and a sinuous appearance. The heterocyst shapes ranged from oval to globular to elongate-barrel, and terminal heterocysts were also linked to frayed filaments, indicating
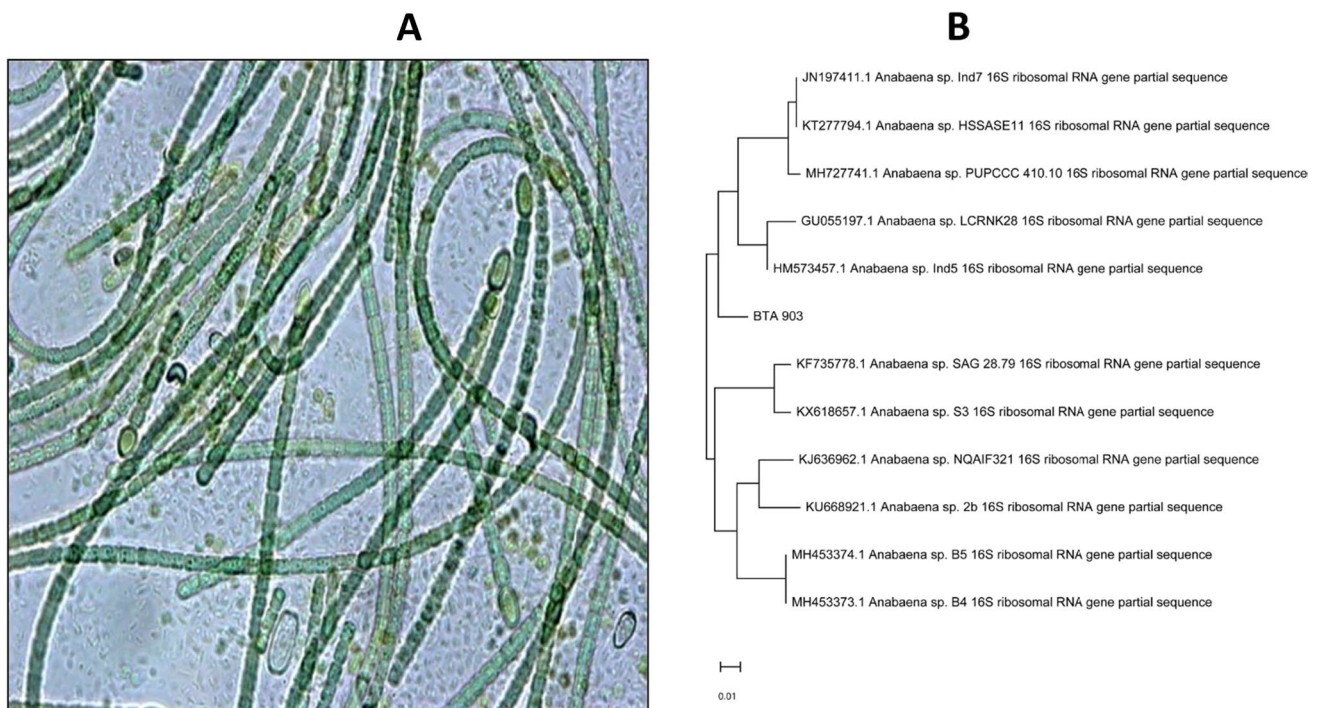
Fig. 1 (**A**) BTA-903 isolate's microscopic appearance, and (**B**) phylogenetic tree depicting the relationships between BTA-903 isolate partial 16S rRNA sequences

that the BTA 903 is *Anabaena sp*. According to Nath et al., (2021), *Anabaena* sp.'s structure has distinct demarcations and a diverse distribution of niche arrays [19]. Microscopic examination revealed a distinct biological feature that explains its unique metabolic processes. *Anabaena* sp. has a high structural and physiological complexity level and occupies a wide range of niches in terrestrial, freshwater, and marine environments [19].

For molecular characterization of BTA 903, genomic DNA was extracted, and this cyanobacterium's consensus 16S rDNA sequences was amplified using PCR. The amplified gene was loaded in agarose gel, and only one 897 base pair band was found for BTA 903. The forward and reverse primers were universal and were used for PCR amplicon amplification. The amplification-derived 16S rDNA gene sequence of BTA 903 was deposited in the NCBI GenBank database with the accession number of KJ652540. The consensus sequence of BTA 903 was compared using the BLAST program to the available sequences of cyanobacterium in the NCBI Genbank database. MEGA 7 software created a phylogenetic tree using the neighbour-joining method, as shown in Fig. 1B [27]. A bootstrap consensus tree inferred from 1000 replicates was used to represent the evolutionary history [28]. The evolutionary distances of BTA 903 were computed using Kimura 2-parameter method. The units of the number of base substitutions per site represent evolutionary distances between BTA 903 and its ancestors [29]. From molecular characterization, it is found that cyanobacterium BTA 903 is *Anabaena sp*. after phylogenetic analysis.

3.2 Determination of the optimum level of glycine, sodium glutamate, light intensity, and photoperiod on biomass and PE production

Cyanobacteria produce PE via a de novo biosynthesis pathway that can be aerobic or anaerobic in nature. δ-Aminolevulinate (ALA) is the first committed precursor of PE and can be synthesized via either the C4 or C5 pathways. ALA synthase produces ALA from glycine in the C4 pathway [30]. Furthermore, glycine provides the carbon atoms for the PE nucleus. As a result, glycine in the medium is expected to regulate the growth of BTA 903 and PE production. The experiments were conducted to determine the role of glycine in BG media on the growth of BTA 903 and PE productivity. Therefore, 0.1 M, 0.2 M, 0.3 M, and 0.4 M glycine concentrations were separately added to BG 11 medium and inoculated with *Anabaena sp*. BTA 903. The incubation temperature of the incubator was maintained at 28 °C for 30 days with a light intensity of 4 k Lux and a day/night ratio of 12:12. Figure 2 a depicts the biomass concentration of BTA 903 as well as the production of PE at various glycine levels. The results show that the growth and production of PE increase

with increasing glycine concentration up to 0.3 M for BTA 903. There was no significant increase in biomass and PE yield as glycine concentration was increased further. Because each cyanobacteria requires an optimal level of nutrients for growth and product formation, 0.3 M of glycine in BG 11 media is thought to be optimal for maximum growth and PE yield. Tiwari et al. (2019) investigated the role of glycine on PE production from *Oscillatoria* sp. while glycine was supplemented in BG 11 media and found similar findings [26]. After 30 days of cultivation, the maximum yields of biomass and C-phycoerythrin (PE) from BTA 903 were 0.912 g/l and 45.57 mg/l, respectively, when 0.3 M of glycine was additionally supplemented in BG 11 media.

The role of sodium glutamate was investigated by varying concentrations of it in BG liquid media containing 0.3 M glycine. In BG 11 liquid media, sodium glutamate concentrations were 2.5 M, 5 mM, 7.5 mM, and 10 mM. BTA 903 was incubated for 30 days at 28 °C in a rotary shaker with the light intensity and photoperiod set to 4 k Lux and 12:12 day-night ratio, respectively. Figure 2 b depicts the biomass yield as well as the production of PE under various glutamate concentrations. The results show that glutamate concentration influences BTA 903 growth and PE accumulation. The first committed precursor for cyanobacterial PE synthesis is ALA. In the C5 pathway, three enzymes are involved in the production of ALA from glutamate [30]. The N atoms in the tetrapyrrole nucleus of PE are supplied by glutamate. The biomass and PE production yield for BTA 903 increases with increasing glutamate concentration up to 5 mM. However, increasing the glutamate concentration further reduces both biomass yield and PE production. Because each cyanobacterium has its own micronutrient requirements for growth and pigment yield, 5 mM of sodium glutamate was optimal for BTA 903 to achieve higher biomass and PE yields. A similar dependence on sodium glutamate was observed for PE accumulation and BTA 170 growth [26]. According to Wanner et al. (1986), the level of expression of PE-encoding genes in cyanobacteria is modulated by the availability of various nutrients in the media [31]. After 30 days of cultivation, 1 g/l of cyanobacterial biomass and 50.45 mg/l of PE were obtained when 0.3 M of glycine and 5 mM of glutamate were added to BG 11 media.

The role of light intensity on the growth of BTA 903 and the accumulation of PE was investigated at varied intensities of light when the incubation was carried out for 30 days. The light intensity was set to 4 k Lux, 6 k Lux, and 8 k Lux. The temperature and photoperiod were kept constant at 28 °C and 12:12 h of day/night, respectively. 0.3 M of glycine and 5 mM of glutamate were supplemented in BG 11 media. Figure 2 c depicts the concentration of BTA 903 biomass and PE concentration after 30 days of cyanobacterial incubation. The results show that growth and PE accumulation increase as light intensity increases from 4 to 6 k Lux. However,
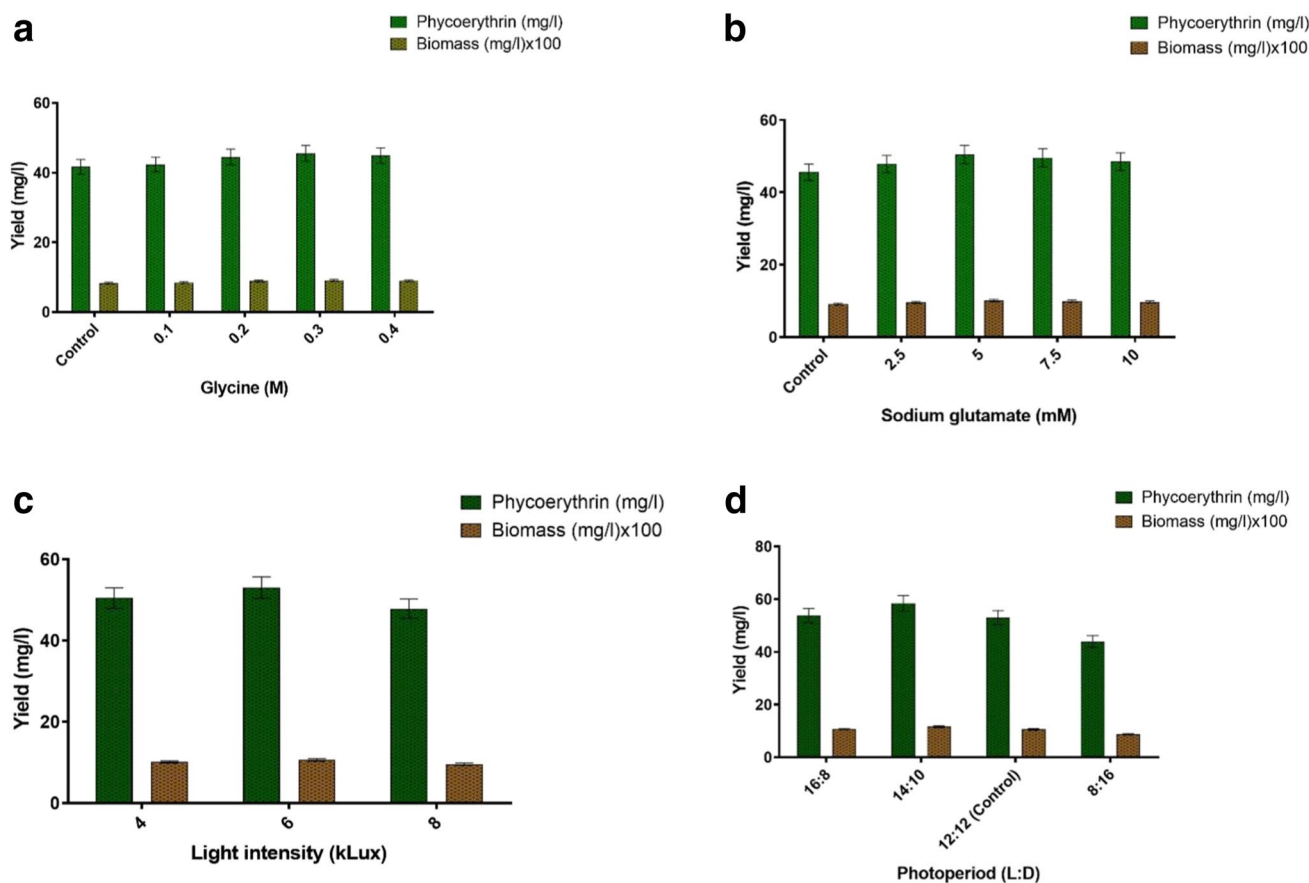
Fig. 2 The role of (**a**) glycine, (**b**) sodium glutamate, (**c**) light intensity, and (**d**) photoperiods on PE and biomass production by BTA-903

when the light intensity was increased further, there was a significant reduction in biomass and PE biosynthesis. Light stress causes photo-oxidative damage to cyanobacterium's photosynthetic machinery and thus has an indirect effect on the growth and accumulation of PE [32]. Bryant et al. (1981) revealed that light intensity influenced the controlled synthesis of light-harvesting phycobiliprotein. Furthermore, light intensity regulates the expression of various subunits of light-harvesting phycobiliprotein [33]. Because genes involved in cyanobacterial growth and pigment accumulation are regulated by light intensity [33], 6 k Lux is regarded as the optimum level of light intensity for achieving higher levels of biomass production and PE accumulation. Tiwari et al. (2019) investigated the role of light intensity on PE production from *Oscillatoria* sp. and found similar findings [26]. After 30 days of cultivation, the maximum biomass and PE yields were 1.06 g/l and 53 mg/l, respectively, when 0.3 M of glycine and 5 mM of glutamate were supplemented in BG 11 media.

The photoperiod is regarded as a critical factor influencing the growth of cyanobacteria along with pigment accumulation [34, 35]. The photoperiod of light clearly regulates the level of composition within the cyanobacteria [36]. The

photoperiod of light condition was varied in this experiment to comprehend the role of photoperiod on the growth of BTA 903 and the production of PE, while light intensity and incubation temperature were kept at 6 k Lux and 28 °C, respectively. The photoperiod of light was kept at 12:12 for light and dark, 14:10 for light and dark, and 8:16 for light and dark. Figure 2 d depicts the biomass and PE yields. The biomass content and PE yield of BTA 903 increased from 0.88 to 1.17 g/L and 44 to 58.45 mg/L, respectively, when the photoperiod was altered from 8:16 (light:dark) to 14:10 (light:dark). When the photoperiod was shifted from 14:10 to 16: 8 of light and dark, the biomass concentration decreased from 1.17 to 1.07 g/L and the PE yield reduced from 58.45 to 53.77 mg/L, respectively. Because the photoperiod of 14:10 (light:dark) produced the highest yield of biomass and PE yield, it is considered optimal. Tiwari et al. (2019) conducted similar research and found that BTA 170 biomass concentration increased to 2.9 from 2.07 g/L, when the photoperiod was altered to 14:10 (light:dark) from 8:16 (light:dark) [26]. The BTA 170 biomass concentration decreased when the photoperiod of light was altered from 14:10 of light and dark to 16:8 of light and dark. Tiwari et al. (2019) made a similar observation when studying the role of

photoperiod on PE accumulation [26]. After 30 days of cultivation, the maximum biomass and PE yields were 1.17 g/L and 58.45 mg/L, respectively, when 0.3 M of glycine and 5 mM of glutamate were supplemented in BG 11 media.

3.3 Batch kinetic study

The prior studies show that various media supplements, such as glycine and sodium glutamate levels, and process conditions, such as light intensity and photoperiod, can influence both BTA 903 and PE production growth. As a result, during the batch kinetics study, BTA 903 was inoculated in 100 ml BG 11 liquid media. However, additional supplements of 0.3 M glycine and 5 mM sodium glutamate were added to the BG 11 media. The batch kinetics study was conducted for 30 days at 28 °C. The light intensity and photoperiod maintained during the batch kinetics study were 6 k Lux and 14:10 light and dark, respectively. Figure 3 a depicts the amounts of biomass and PE produced. When looking at the growth curves of BTA 903, three distinct phases are visible: lag, log, and stationary. Figure 3 a shows that the BTA 903 growth curve lag phase was observed for two days after inoculation in BG 11 liquid media. However, the log and stationary phases were extended for 18 and 10 days, respectively. When studying the growth of cyanobacteria, Tiwari et al. (2019) made a similar observation [26]. The biomass productivity of *Anabaena* sp. BTA 903 was estimated to be 39 mgL^{-1} day^{-1}. Based on log phase data, the specific growth rate of BTA 903 was calculated and found to be 0.150 day^{-1}. For BTA 903, the doubling time was estimated to be 4.6 days. The specific growth rate of *Oscillatoria sp.* is found to be 0.206 day^{-1}, which is higher than the *Anabaena* sp. BTA 903 [26]. Figure 3 a shows that during the log phase, the rate of PE production increased as the biomass of BTA 903 increased. Furthermore, sufficient PE yield was observed in the stationary phase. A contradictory observation was made while evaluating the kinetics of PE production in *Oscillatoria* sp. in BG 11 media [26]. Tiwari et al. (2019) reported that the PE production rate is prominent in the log phase, but there is no significant increase in the the stationary phase [26]. After 30 days of cultivation, the PE and biomass production yields were 58.45 mgL^{-1} and 1.17 gL^{-1}, respectively.

PE production patterns were examined using the Leudeking-Piret (LP) model, as shown in Eq. (3). Equations (1) and (2) were used to calculate the specific growth and production rates, respectively. Figure 3 b depicts the relationship between the specific PE production rate and the specific growth rate. According to Fig. 3 b, the growth-associated constant (α) and non-growth-associated constant (β) for PE were determined to be 0.0027 and 0.0024, respectively. The results show that PE was produced in both log phase and the stationary phase. Tiwari et al. (2019) reported that
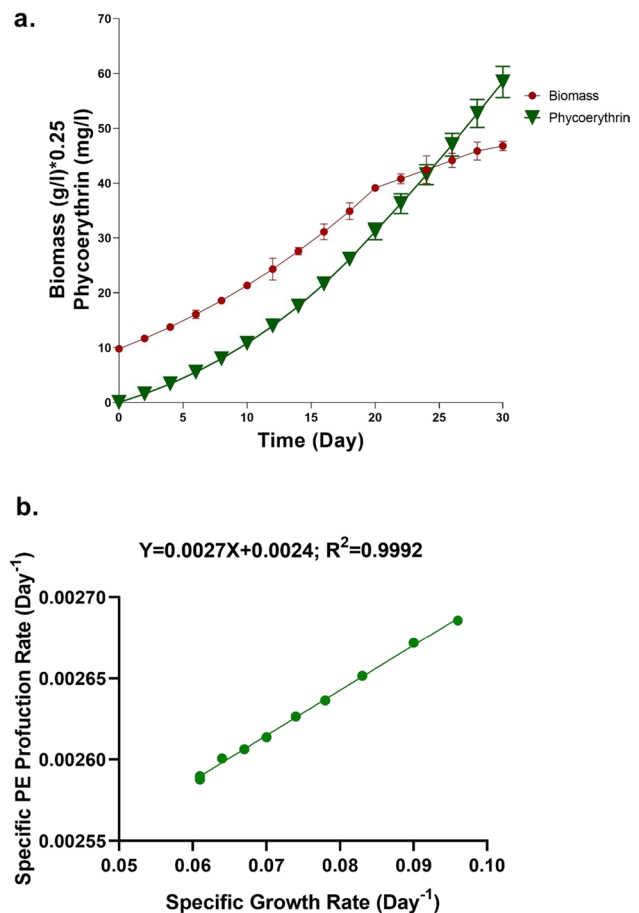
Fig. 3 (**a**) Time-dependent profile of biomass, and C-phycoerythrin (PE) production by BTA-903, and (**b**) relation between specific PE production rate vs. specific BTA 903 growth rate

PE production is associated with growth, while PE production from *Oscillatoria* sp. was studied in BG 11 media [26]. The value of growth associated (α) and nongrowth associated (β) constants for PE were found to be 0.114 and zero, respectively, for *Oscillatoria* sp. In the present studies, it is evident that PE is a secondary metabolite for BTA 903. Table 1 summarizes the current state of phycoerythrin production in various cyanobacteria. However, after 30 days of cultivation, BTA 903 can produce 58.45 mgl^{-1} of PE. Since *Anabaena* sp. has significantly more PE than other cyanobacterial strains reported in the literature, commercial production of PE from this strain is possible to meet the industry's demand for PE.

3.4 Analysis of BTA 903 composition, PBPs, chlorophyll-a, ammonia excretion of BTA 903

To determine ash, carbohydrate, protein, lipid, and moisture content in *Anabaena* sp., 1.631 g of lyophilized BTA 903 was used in this experiment. *Anabaena* sp. is made up of

Table 1 The level of phycoerythrin found in various cyanobacteria

SL. No	Name of the strains	Phycoerythrin	Reference
1	*Nostoc* sp.	65.04 µg/mL	[46]
2	*Oscillatoria* sp. BTA170	62.54 mg/L	[26]
3	*Anabaena* CCC 744	12.39 µg/mg	[19]
4	*Pseudanabaena* sp.	39.2 mg/L	[47]
5	*Oscillatoria* sp.	31.25 mg/g	[48]
6	*Pseudanabaena* sp.	14.9 mg/L	[47]
7	*Porphyridium* sp. CCAP 1380	33.85 mg/g	[49]
8	*Nostoc* sp. HKAR-2	0.105 mg/mL	[50]
9	*Nostoc* sp. PACC-8205	0.018 mg/mL	[51]
10	*Nostoc* sp. PACC-8646	0.035 mg/mL	[51]
11	*Lyngbya* sp. CCNM 2053	22.99 ± 0.52 mg/g	[52]
12	*Pseudanabaena* sp.	32.2 mg/L	[47]
13	*Microcoleus autumnalis* PACC-5505	0.132 mg/mL	[51]
14	*Microcoleus autumnalis* PACC-5522	0.201 mg/mL	[51]
15	*Microcoleus autumnalis* PACC-5527	0.136 mg/mL	[51]
16	*Microcoleus autumnalis* PACC-5511	0.106 mg/mL	[51]
17	*Anabaena* sp. PACC-8632	0.069 mg/mL	[51]
18	*Anabaena* sp. BTA 903	49.96 ± 1.46 mg/g	Present study

a variety of components which are either organic or inorganic. Because the lyophilized form was used to determine the composition in BTA 903, it is obvious that the moisture percentage will be attributed. The inorganic components of BTA 903 were analysed by the determination of ash content, which was performed at 550 °C in a furnace. Figure 4 a depicts the major cellular constituents of *Anabaena* sp. It contains 5.84% (w/w) ash, 42.36% (w/w) carbohydrate, 33.46% (w/w) protein, 16.46% (w/w) lipid, and 1.88% (w/w) moisture, as shown in Fig. 4 a. Nath et al. (2021) investigated the different cellular contents of 1.545 g of lyophilized *Anabaena* sp. CCC 744[19]. They found that lyophilized CCC 744 contained 6.61%, 26.10%, 38.57%, 27.13%, and 1.6% ash, carbohydrate, protein, lipid, and moisture, respectively. According to their research, it is reported that the major component of CCC 744 was protein, followed by lipid and carbohydrate [19]. According to the present findings, carbohydrate is the most important cellular component, followed by protein and lipid. The availability of major components within cyanobacteria is affected by strain type, environmental parameters, and the method used to determine components. The correct strain for any industrial application must be chosen after analysing the level of major components present within cyanobacteria, as major components are not fixed for any type of strain. Since *Anabaena* sp. BTA 903 contains 42.36% carbohydrate and 16.46% lipid, the strain is more suitable for industrial bioethanol and biodiesel production. However, a high carbohydrate content can be beneficial in producing chemicals. Furthermore, as it contains 33.46% protein, BTA 904 can be used in animal feed and as a source of various bioproducts.

The levels of phycobiliproteins (PBPs) such as C-phycocyanin (PC), along with allophycocyanin (APC), and C-phycoerythrin (PE) were measured after 30 days of cultivation of *Anabaena* sp. BTA 903. PE production was found to be highest among PBPs, followed by APC and PC (Fig. 4b). After 30 days of cultivation in a previously optimized medium, 49.96 mg PE/g biomass, 27.53 mg PC/g biomass, and 30.39 mg APC/g biomass were produced. Environmental factors, as well as nutritional parameters, can affect the physiology and biosynthesis of pigments, resulting in variation in dye production within species. Chlorophyll-a is a pigment used by cyanobacteria to collect solar energy for photosynthesis. The chlorophyll-a production was found to be 6.9 mg/g of biomass after 30 days of cultivation of *Anabaena sp*. BTA 903 in previously optimized media (Fig. 4b). According to Nath et al., (2021), the content of chlorophyll-a was measured as 2.98 and 7.44 g/mg of biomass after fifteen and thirty days of incubation in BG 11 media, respectively [19]. Chlorophyll-a concentrations may be increasing due to changes in irradiation or cell density [37]. Since the growth of all of the cells tool place under constant illumination, the current investigation concludes that decreasing the density of cell is the cause of the lower level of chlorophyll-a. Many cyanobacterial strains are capable of nitrogen fixation. The ability to fix nitrogen results in diazotrophic cyanobacteria that can survive in nitrogen-limiting environments [38]. The cyanobacterial species that are frequently used in the field as green manure replace synthetic manure [39]. *Anabaena* sp. develops heterocysts, a type of cell known for nitrogen fixation, under nitrogen-depleted conditions. The nitrogen fixation enzyme nitrogenises fixes nitrogen from the air.
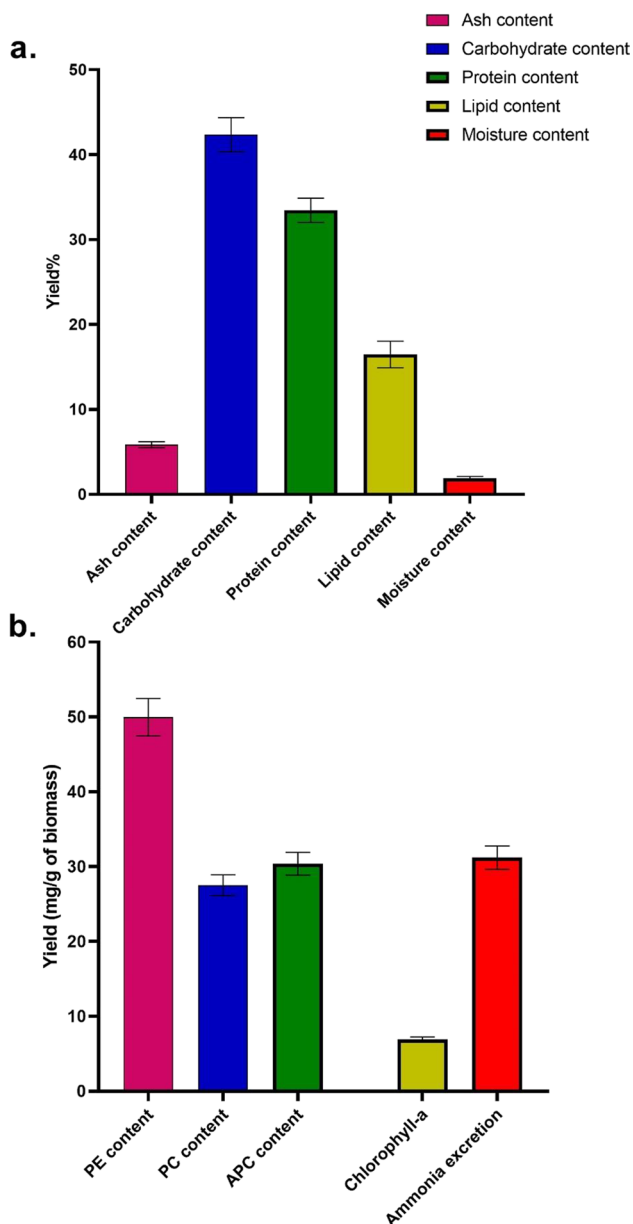
Fig. 4 **a**) Comparison of cellular components including ash, carbohydrate, protein, lipid, moisture, and **b**), PE, PC, APC, chlorophyl- a, and ammonia excretion of BTA-903

Ammonia is considered a nitrogen reserve (inorganic) primarily used by most cyanobacteria [40]. Ammonia appears to be an essential intracellular intermediate of nitrogen-fixer strains for nitrogen integration [41]. *Anabaena* sp. BTA 903's ammonia excretion competence was investigated after inoculating the strain in previously optimized media and withdrawing samples after thirty days of incubation. Figure 4 b depicts the content of ammonia excretion found after 30 days of incubation. The amount of ammonia excretion was found to be 31.2 mg/g of biomass. To investigate the ammonia excretion capability of *Anabaena* sp. CCC 744,

Nath et al., (2021) inoculated the strain in BG 11 liquid media and collection of the samples was carried out after fifteen and thirty days of incubation [19]. They revealed that as the incubation time of CCC 744 was increased, the amount of ammonia excretion increased, reaching 12.3 g/mg after 15 days and 33.7 g/mg after 30 days, respectively.

3.5 Thermodynamics and stability of PE

PE deactivation studies were carried out under various pH and temperature conditions. The deactivation of PE is assumed to follow first-order kinetics.

$$P_{APE} \rightarrow P_{DPE} \qquad (4)$$

P_{APE} denotes an active PE that is directly transformed into an inactive state P_{DPE}. It is presumed that no intermediates are developed during the deactivation phase. The deactivation process is denoted as:

$$\frac{dP_{APE}}{dt} = -k_d[P_{APE}] \qquad (5)$$

The k_d denotes PE deactivation rate constant. After integrating of Eq. (5) yields Eq. (6)

$$a = exp\left(-k_d^t\right) \qquad (6)$$

where, $a = \frac{P_{DPE}}{P_{APE}}$

After plotting ln (α) versus t, slope was used to calculate k_d. Equation (7) was used to calculate the half-life ($t_{1/2}$) of PE. The time required for 50% deactivation of PE is defined as its half life.

$$t_{1/2} = \frac{ln2}{k_d} = \frac{0.693}{k_d} \qquad (7)$$

Table 2 shows the calculated deactivation rate constants for PE under various conditions. Table 2 shows that the deactivation of PE is prominent in the presence of various temperatures and pH. When experiments were carried out at a particular pH, the k_d values of PE increased as the temperature went up. Protein integrity is maintained by the orientation of its secondary, tertiary, and quaternary structures. When the structure of a protein changes, it deactivates due to changes in its environment [26]. The functional property, as well as stability analysis of purified PE, was conducted by Rastogi et al. (2015), where various temperatures and pH were used [42]. They looked into the stability of purified PE in different environments. The role of pH and temperature on PE stability was investigated separately in their study; however, the synergistic role of these factors on PE has yet to be explored properly. When incubated at 80 °C for 1 h, they found that 84.33% of the PE remained active. When incubated at pH 12 for 1 h, the residual fraction of PE was found to be 60.86%

Table 2 The role of temperature and pH on the deactivation rate constant (k_d) of PE

Temp. (^{o}C)	Deactivation rate constant (k_d, hr^{-1})						
	pH (2)	pH (4)	pH (6)	pH (7)	pH (8)	pH (10)	pH (12)
10	0.443	0.232	0.115	0.000	0.167	0.257	0.473
20	0.457	0.247	0.130	0.001	0.182	0.273	0.488
30	0.472	0.260	0.144	0.010	0.195	0.286	0.503
37	0.483	0.272	0.155	0.062	0.207	0.297	0.512
40	0.504	0.293	0.177	0.115	0.228	0.319	0.534
50	0.536	0.324	0.208	0.135	0.260	0.351	0.566
60	0.555	0.345	0.228	0.155	0.280	0.371	0.587
70	0.582	0.371	0.255	0.178	0.307	0.397	0.612
80	0.641	0.431	0.313	0.200	0.365	0.456	0.671

[42]. Tiwari et al. (2019) studied the stability of PE in the presence of temperature and pH [26]. They reported that the deactivation rate constants for PE were zero when stability analysis was performed in the temperature range of 10–40 °C and pH of 7. Almost identical findings in the temperature range of 10–30 °C were made in the current studies. The deactivation rate constants for PE at pH 7 were determined to be 0.062 and 0.115 at 37 °C and 40 °C, respectively. Furthermore, when compared to other pHs tested at the same temperature, the lowest k_d value for PE was found at pH 7, which various researchers also observed. The deactivation process for crude PE is faster at high alkaline pH than at acidic pH. It was found that pH 12 is more detrimental to PE, and the highest k_d value (0.671) was obtained when the experiment was conducted at 80 °C. After 1 h of incubation at pH 12 and 80 °C, it was found that PE retained 51.10% of its active concentrations [26]. Tiwari et al. (2019) reported a nearly identical observation, with 56.8% of PE remaining active after a 1-h incubation at pH 12 and 80 °C [26]. Electrostatic and hydrogen bonds are the two types of bonds that maintain protein structures. If these bonds in PE structure are disrupted due to environmental changes, protein deactivation occurs [26]. Equation (7) was used to calculate the effect of temperature on half-life time at various pH levels. When the investigation was carried out within the range of 10 to 80 °C and a specific pH, the half-life of PE decreased as temperature increased. It is also clear that the decay of the half-life of PE is faster in alkaline conditions than in acid environments. When crude PE was studied at temperatures of 80 °C and pH 12, it showed the shortest half life (1.03 h), indicating that PE is more unstable at these temperatures and pH levels. Tiwari et al. (2019) revealed the shortest half-life (1.22 h) of crude PE at 80 °C and pH 12 [26]. Protein stability is determined by various structures and bonds, such as electrostatic and hydrogen bonds. As a result, the half-life value varies when studied at different pH and temperature levels [26].

In the deactivation study, various thermodynamic parameters were measured to evaluate the mechanism of PE deactivation process. Initially, entropy (ΔS^*) and enthalpy (ΔH^*)

were measured, followed by Gibb's free energy (ΔG^*) and activation energy (E_a) of the biochemical process [43]. The relationship between temperature and the deactivation rate constant is shown as:

$$k_d = \frac{kT}{h} e^{\left(\frac{\Delta S^*}{R}\right)} e^{\left(\frac{-\Delta S^*}{RT}\right)} \quad (8)$$

Or

$$\text{In}\left(\frac{k_d}{T}\right) = \text{In}\left(\frac{k}{h}\right) + \frac{\Delta S^*}{R} - \frac{\Delta H}{RT} \quad (9)$$

ΔH^* and ΔS^* are represented as enthalpy and entropy, respectively. R and T are gas constant and absolute temperature, respectively. Plank's constant is denoted as h, and Boltzmann's constant is represented as 'k'. After plotting ln (k_d/T) versus 1/T, the values of enthalpy and entropy were computed.

The following Eq. (10) was used for calculation of Gibb's free energy $(\Delta G*)$

$$\Delta G^* = \Delta H^* - T\Delta S^* \quad (10)$$

The Arrhenius equation was used to calculate activation energy (E_a) from Eq. (11).

$$k_d = k_0 e^{\left(\frac{E_a}{RT}\right)} \quad (11)$$

Or

$$\text{In}(k_d) = \text{In}(k_0) - \left(\frac{E_a}{R}\right)\frac{1}{T} \quad (12)$$

The frequency factor is denoted by k_0, calculated by plotting ln (k_d) against 1/T. The activation energy value was also calculated using the same graph. Table 3 shows the values of various thermodynamic parameters like enthalpy and entropy of crude PE at different pH levels. The values of H* and S* are affected by the solvent and structural effects of PE. Entropy is commonly used to represent the randomness or disorder in protein structure. Protein deactivation

occurs due to a change in the interaction of the protein and the solvent, which is measured by entropy. Positive entropy values indicate higher order of disorder in the system and are responsible for the deactivation or denaturation of PE. Negative entropy values, on the other hand, support higher stability by indicating a low level of randomness in the system [44]. Table 3 shows that the entropy values for PE are negative at all experimented pH ranges. The results show that PE is more compact in all tested pHs, resulting in less disorder in the PE molecule [43, 45]. The entropy value was found to be -313.69, -308.7, -298.40, -299.74, -304.50, -309.80, and -313.90 at pH 2, 4, 6, 8,0, and 12, respectively. Tiwari et al. (2019) found a similar observation, and the value of entropy (-198.90 J/mol K) was found to be minimum at pH 7 [26]. Enthalpy represents the quantity of energy needed for the denaturation process of PE. As a result, higher-order PE stability is denoted by a greater value of deactivation process enthalpy [44]. The maximum values of enthalpy for PE were revealed at pH 7 and calculated as 9.88 kJ/mol. Enthalpy was found to be the lowest (1.45 kJ/mol) at pH 12. More acidic and alkaline environments reduce the enthalpy of the PE deactivation process. Because of the compactness of the PE structure, the negative entropy and positive enthalpy values found in all tested pHs are suitable for PE stability [43]. Tiwari et al. (2019) found a similar observation, with the maximum value of enthalpy (47.13 kJ/mol) found at pH 7 [26].

A higher order of S* indicates that more PE molecules have entered a transition state, resulting in a lower value of G*. G* is an essential thermodynamic parameter to assess protein stability rather than entropy and enthalpy because it results from entropy and enthalpy changes. The value of G* was calculated for PE at various pHs and temperatures and is given in Table 3. Table 3 shows that the calculated G* value of PE is positive for all pHs tested, implying that the PE is stable mainly in the above environmental conditions. At pH 7, PE had a higher Gibb's free energy (103.70–115.69 kJ/mol), indicating that it is mostly stable. Tiwari et al. (2019) revealed a similar result, with the highest value of Gibb's free energy (109.38–117.34 kJ/

mol) observed at pH 7 [26]. Equation (11) represents the Arrhenius equation, from which the changes in k_d with temperature can be calculated. The activation energy (E_a) was calculated after plotting $\ln(k_d)$ and 1/T, and the value of k_0 was also computed using the same plot. E_a calculated at pH 7 was found to be 9.88 kJ/mol, higher than the other tested pH for PE. In particular, the higher the activation energy, the slower the deactivation of PE. Tiwari et al. (2019) revealed a similar result, with the highest value of activation energy (49.89, kJ/mol) observed at pH 7 [26].

4 Conclusion

Cyanobacterium BTA 903, isolated from Manipur, India, was identified as *Anabaena* sp. based on morphological identification and phylogenetic analysis. Cyanobacterium cellular components have a high carbohydrate, protein, and lipid content, indicating they could be used as feedstock in various industrial applications. PE production is found to be associated with mixed growth. The amount of glycine and sodium glutamate in the media and the appropriate light intensity and photoperiod influences PE biosynthesis. *Anabaena* sp. produced chlorophyll-a, phycobiliproteins (PBPs), and ammonia excretion, which can be used in various manufacturing applications. Temperature and pH are essential factors in the deactivation of PE. Compared to other pHs at specific temperatures, pH 7 had the lowest k_d value of PE. Furthermore, the deactivation process for crude PE was found to be faster at high alkaline pH compared to acidic pH. Higher acidic and basic conditions are responsible for lowering the value of entropy and enthalpy for PE. PE had higher positive G* values in all tested pHs, indicating that PE is mostly stable across the pH and temperature ranges tested. When all tested pHs were compared, G* values in pH-7 were found to be more favourable for PE. According to the findings, BTA 903 can be used as a feedstock and for producing PE in the industry.

Table 3 The values of thermodynamic properties during PE thermal deactivation

pH	Enthalpy (H^*) (kJ.mol^{-1})	Entropy (S^*) (J/mol K)	Activation energy (E_a), (kJ.mol^{-1})	Frequency factor (k_0), (sec^{-1})	Gibb's free energy (G*) (kJ. mol^{-1})
2	1.67	-313.69	4.3	73X10^{-5}	90.44–112.40
4	4.65	-308.7	7.2	134X10^{-5}	92–113.62
6	9.22	-298.40	11.85	463X10^{-5}	93.67–114.56
7	9.88	-299.74	12.64	414X10^{-5}	103.70–115.69
8	6.57	-304.50	9.25	222X10^{-5}	92.74–114
10	4.08	-309.80	6.71	117X10^{-5}	91.76–113.44
12	1.45	-313.90	4.08	71X10^{-5}	90.29–112.26

Data availability The data generated or obtained during the experiment for this study is available to the associated author (Pinku Chandra Nath) and can be made available to this journal at a reasonable cost upon request.

Declarations

Ethics approval This article contains no studies with human or animal participants conducted by any authors.

Consent to participate Informed consent was obtained from all individual participants included in the study.

Consent for publication The authors confirm that all data in the manuscript were provided with informed consent by human research participants.

Competing interests The authors declare no competing interests.

References

1. Mercier L, Peltomaa E, Ojala A (2022) Comparative analysis of phycoerythrin production in cryptophytes. J Appl Phycol 34(2):789–797. https://doi.org/10.1007/s10811-021-02657-z

2. Latsos C, van Houcke J, Blommaert L, Verbeeke GP, Kromkamp J, Timmermans KR (2021) Effect of light quality and quantity on productivity and phycoerythrin concentration in the cryptophyte *Rhodomonas sp*. J Appl Phycol 33(2):729–741. https://doi.org/10.1007/s10811-020-02338-3

3. Sargazi S, Fatima I, Kiani MH, Mohammadzadeh V, Arshad R, Bilal M, Rahdar A, Díez-Pascual AM, Behzadmehr R (2022) Fluorescent-based nanosensors for selective detection of a wide range of biological macromolecules: a comprehensive review. Int J Biol Macromol 206:115–147. https://doi.org/10.1016/j.ijbiomac.2022.02.137

4. Siddiki SYA, Mofijur M, Kumar PS, Ahmed SF, Inayat A, Kusumo F, Badruddin IA, Khan TY, Nghiem L, Ong HC (2022) Microalgae biomass as a sustainable source for biofuel, biochemical and biobased value-added products: an integrated biorefinery concept. Fuel 307:121782–121791. https://doi.org/10.1016/j.fuel.2021.121782

5. Balaraman HB, Sivasubramanian A, Rathnasamy SK (2021) Sustainable valorization of meat processing wastewater with synergetic eutectic mixture based purification of R-Phycoerythrin from porphyrium cruentium. Biores Technol 336:125357–125368. https://doi.org/10.1016/j.biortech.2021.125357

6. Seručnik M, Vicente FA, Zi B, JoA C, SnP V, Žnidaršič-Plazl P (2020) Development of a microfluidic platform for R-phycoerythrin purification using an aqueous micellar two-phase system. ACS Sustain Chem Eng 8(46):17097–17105. https://doi.org/10.1021/acssuschemeng.0c05042

7. Ulagesan S, Nam T-J, Choi Y-H (2021) Extraction and purification of R-phycoerythrin alpha subunit from the marine red algae pyropia yezoensis and its biological activities. Molecules 26(21):6479–6491. https://doi.org/10.3390/molecules26216479

8. Castro-García SZ, Chamorro-Cevallos G, Quevedo-Corona L, McCarty MF, Bobadilla-Lugo RA (2018) Beneficial effects of phycobiliproteins from *Spirulina* maxima in a preeclampsia model. Life Sci 211:17–24. https://doi.org/10.1016/j.lfs.2018.09.011

9. Nath PC, Bandyopadhyay TK, Mahata N, Pabbi S, Tiwari ON, Indira M, Bhunia B (2022) Optimization and kinetic study of ultrasonic-mediated phycoerythrin extraction from *Anabaena sp*. Biomass Convers Biorefin 12:1–12. https://doi.org/10.1007/s13399-022-03329-9

10. Mahanil K, Sensupa A, Pekkoh J, Tragoolpua Y, Pumas C (2021) Application of phycobiliproteins from *Leptolyngbya sp*. KC45 for natural illuminated colourant beverages. J Appl Phycol 33:3747–3760. https://doi.org/10.1007/s10811-021-02556-3

11. Nowruzi B, Konur O, Anvar SAA (2022) The Stability of the phycobiliproteins in the adverse environmental conditions relevant to the food storage. Food Bioprocess Technol 15:2646–2663. https://doi.org/10.1007/s11947-022-02855-8

12. Galetović A, Seura F, Gallardo V, Graves R, Cortés J, Valdivia C, Núñez J, Tapia C, Neira I, Sanzana S (2020) Use of phycobiliproteins from atacama cyanobacteria as food colorants in a dairy beverage prototype. Foods 9:244–253. https://doi.org/10.3390/foods9020244

13. Pereira T, Barroso S, Mendes S, Gil MM (2020) Stability, kinetics, and application study of phycobiliprotein pigments extracted from red algae *Gracilaria gracilis*. J Food Sci 85(10):3400–3405. https://doi.org/10.1111/1750-3841.15422

14. Ma J, Hu J, Sha X, Meng D, Yang R (2022) Phycobiliproteins, the pigment-protein complex form of natural food colorants and bioactive ingredients. Crit Rev Food Sci Nutr 4:1–19. https://doi.org/10.1080/10408398.2022.2128714

15. Stanier R, Kunisawa R, Mandel M, Cohen-Bazire G (1971) Purification and properties of unicellular blue-green algae (order Chroococcales). Bacteriol Rev 35:171–205. https://doi.org/10.1128/br.35.2.171-205.1971

16. Rastogi RP, Kumari S, Han T, Sinha RP (2012) Molecular characterization of hot spring cyanobacteria and evaluation of their photoprotective compounds. Can J Microbiol 58(6):719–727. https://doi.org/10.1139/w2012-044

17. Altschul SF, Gish W, Miller W, Myers EW, Lipman DJ (1990) Basic local alignment search tool. J Mol Biol 215:403–410. https://doi.org/10.1016/S0022-2836(05)80360-2

18. Kandeel M, Mohamed ME, Abd El-Lateef HM, Venugopala KN, El-Beltagi HS (2022) Omicron variant genome evolution and phylogenetics. J Med Virol 94(4):1627–1632. https://doi.org/10.1002/jmv.27515

19 Nath PC, Tiwari ON, Devi I, Bandyopadhyay TK, Bhunia B (2021) Biochemical and morphological fingerprints of isolated Anabaena sp: a precious feedstock for food additives. Biomass Convers Biorefin 11(6):2723–2733. https://doi.org/10.1007/s13399-020-00651-y

20. Bennett A, Bogorad L (1973) Complementary chromatic adaptation in a filamentous blue-green alga. J Cell Biol 58:419–435. https://doi.org/10.1083/jcb.58.2.419

21. Jagannath S, Ramachandran K (2010) Influence of competing metabolic processes on the molecular weight of hyaluronic acid synthesized by *Streptococcus zooepidemicus*. Biochem Eng J 48:148–158. https://doi.org/10.1016/j.bej.2009.09.003

22. Luedeking R, Piret EL (2000) A kinetic study of the lactic acid fermentation. Batch process at controlled pH. Biotechnol Bioeng 67:636–644. https://doi.org/10.1002/jbmte.390010406

23. Kim JH, Choi W, Jeon SM, Kim T, Park A, Kim J, Heo SJ, Oh C, Shim WB, Kang DH (2015) Isolation and characterization of *Leptolyngbya sp.* KIOST-1, a basophilic and euryhaline filamentous cyanobacterium from an open paddle-wheel raceway Arthrospira culture pond in Korea. J Appl Microbiol 119:1597–1612. https://doi.org/10.1111/jam.12961

24. Lowry OH, Rosebrough NJ, Farr AL, Randall RJ (1951) Protein measurement with the Folin phenol reagent. J Biol Chem 193:265–275. https://doi.org/10.1111/jbc.14907713

25. Spiro RG (1966) Analysis of sugars found in glycoproteins. Methods Enzymol 8:3–26. https://doi.org/10.1016/0076-6879(66)08005-4

26. Tiwari ON, Bhunia B, Chakraborty S, Goswami S, Devi I (2019) Strategies for improved production of phycobiliproteins (PBPs) by *Oscillatoria sp. BTA170* and evaluation of its thermodynamic and kinetic stability. Biochem Eng J 145:153–161. https://doi.org/10.1016/j.bej.2019.02.016

27. Saitou N, Nei M (1987) The neighbor-joining method: a new method for reconstructing phylogenetic trees. Mol Biol Evol 4(4):406–425. https://doi.org/10.1093/oxfordjournals.molbev.a040454

28. Felsenstein J (1985) Confidence limits on phylogenies: an approach using the bootstrap. Evolution 39:783–791. https://doi.org/10.1111/j.1558-5646.1985.tb00420.x

29. Kimura M (1980) A simple method for estimating evolutionary rates of base substitutions through comparative studies of nucleotide sequences. J Mol Evol 16:111–120. https://doi.org/10.1007/BF01731581

30. Avissar YJ, Ormerod JG, Beale SI (1989) Distribution of δ-aminolevulinic acid biosynthetic pathways among phototrophic bacterial groups. Arch Microbiol 151:513–519. https://doi.org/10.1007/BF00454867

31. Wanner G, Henkelmann G, Schmidt A, Köst H-P (1986) Nitrogen and sulfur starvation of the *cyanobacterium Synechococcus* 6301 an ultrastructural, morphometrical, and biochemical comparison. Zeitschrift für Naturforschung C 41:741–750. https://doi.org/10.1515/znc-1986-7-814

32. Erickson E, Wakao S, Niyogi KK (2015) Light stress and photoprotection in *Chlamydomonas reinhardtii*. Plant J 82:449–465. https://doi.org/10.1111/tpj.12825

33. Bryant DA (1981) The photoregulated expression of multiple phycocyanin species. FEBS J 119:425–429. https://doi.org/10.1111/j.1432-1033.1981.tb05625.x

34. Khoeyi ZA, Seyfabadi J, Ramezanpour Z (2012) Effect of light intensity and photoperiod on biomass and fatty acid composition of the microalgae, *Chlorella vulgaris*. Aquacult Int 20:41–49. https://doi.org/10.1007/s10499-011-9440-1

35. Oh SH, Han JG, Kim Y, Ha JH, Kim SS, Jeong MH, Jeong HS, Kim NY, Cho JS, Yoon WB (2009) Lipid production in *Porphyridium cruentum* grown under different culture conditions. J Biosci Bioeng 108:429–434. https://doi.org/10.1016/j.jbiosc.2009.05.020

36. Seyfabadi J, Ramezanpour Z, Khoeyi ZA (2011) Protein, fatty acid, and pigment content of Chlorella vulgaris under different light regimes. J Appl Phycol 23:721–726. https://doi.org/10.1007/s10811-010-9569-8

37. Fontes AG, Vargas M, Moreno J, Guerrero MG, Losada M (1991) Changes in the pigment content of *Anabaena* variabilis cells in outdoor culture. J Plant Physiol 137:441–445. https://doi.org/10.1016/S0176-1617(11)80314-7

38. Shiozaki T, Nagata T, Ijichi M, Furuya K (2015) Nitrogen fixation and the diazotroph community in the temperate coastal region of the northwestern North Pacific. Biogeosciences 12:4751–4764. https://doi.org/10.5194/bg-12-4751-2015

39. Parmar A, Singh NK, Pandey A, Gnansounou E, Madamwar D (2011) Cyanobacteria and microalgae: a positive prospect for biofuels. Biores Technol 102:10163–10172. https://doi.org/10.1016/j.biortech.2011.08.030

40. Subramanian G, Shanmugasundaram S (1986) Uninduced ammonia release by the nitrogen-fixing cyanobacterium *Anabaena*. FEMS Microbiol Lett 37:151–154. https://doi.org/10.1111/j.1574-6968.1986.tb01784.x

41. Boussiba S, Gibson J (1991) Ammonia translocation in cyanobacteria. FEMS Microbiol Rev 8:1–14. https://doi.org/10.1111/j.1574-6968.1991.tb04953.x

42. Rastogi RP, Sonani RR, Madamwar D (2015) Physico-chemical factors affecting the in vitro stability of phycobiliproteins from *Phormidium rubidum* A09DM. Biores Technol 190:219–226. https://doi.org/10.1016/j.biortech.2015.04.090

43. Narayana Naidu GS, Panda T (2003) Studies on pH and thermal deactivation of pectolytic enzymes from *Aspergillus niger*. Biochem Eng J 16:57–67. https://doi.org/10.1016/S1369-703X(03)00022-6

44. Marangoni AG (2003) Enzyme kinetics: a modern approach. John Wiley & Sons Inc, NJ

45. Foster RL (1980) The nature of enzymology. Croom Helm, London

46. Nowruzi B, Fahimi H, Lorenzi AS Recovery of pure C-phycoerythrin from a limestone drought tolerant cyanobacterium Nostoc sp. and evaluation of its biological activity. In: Anales de Biología, 2020. vol 42. Servicio de Publicaciones de la Universidad de Murcia, pp 115–128

47. Mishra SK, Shrivastav A, Maurya RR, Patidar SK, Haldar S, Mishra S (2012) Effect of light quality on the C-phycoerythrin production in marine cyanobacteria *Pseudanabaena sp.* isolated from Gujarat coast. India Protein Expr Purif 81:5–10. https://doi.org/10.1016/j.pep.2011.08.011

48. Deviram G, Mathimani T, Anto S, Ahamed TS, Ananth DA, Pugazhendhi A (2020) Applications of microalgal and cyanobacterial biomass on a way to safe, cleaner and a sustainable environment. J Clean Prod 253:119770–119781. https://doi.org/10.1016/j.jclepro.2019.119770

49. Ardiles P, Cerezal-Mezquita P, Salinas-Fuentes F, Órdenes D, Renato G, Ruiz-Domínguez MC (2020) Biochemical composition and phycoerythrin extraction from red microalgae: a comparative study using green extraction technologies. Processes 8:1628–1639. https://doi.org/10.3390/pr8121628

50. Kannaujiya VK, Sinha RP (2016) Thermokinetic stability of phycocyanin and phycoerythrin in food-grade preservatives. J Appl Phycol 28(2):1063–1070. https://doi.org/10.1007/s10811-015-0638-x

51. Basheva D, Moten D, Stoyanov P, Belkinova D, Mladenov R, Teneva I (2018) Content of phycoerythrin, phycocyanin, allophycocyanin and phycoerythrocyanin in some cyanobacterial strains: applications. Eng Life Sci 18:861–866. https://doi.org/10.1002/elsc.201800035

52. Ghosh T, Mishra S (2020) Studies on extraction and stability of C-Phycoerythrin from a marine cyanobacterium. Front Sustain Food Syst 4:102–113. https://doi.org/10.3389/fsufs.2020.00102